Supporting Information

Kopp et al. 10.1073/pnas.0909605107

SI Text

SI Materials and Methods.

Standardization of radiative forcings. To facilitate comparison of different estimates of the contribution of carbonaceous aerosols to global radiative forcing, we convert the reported results of A (1, 2), H (3, 4), RC (5), and J (6–9) into the common terms of effective radiative forcing, including direct, indirect, and snow albedo effects. Where possible (A, H, RC), we adjust the results to use the best estimate of carbonaceous aerosol emissions from ref. 10. Key parameters are shown in Tables S1 and S2.

Models A and H.

We calculate steady-state normalized direct radiative forcings (*ssNDRF*) for A and H based on the reported direct radiative forcings (*DRF*) and the emissions (E) used in the models.

$$ssNDRF_{i,j,k} = DRF_{i,j,k}/E_{i,j,k} \qquad i = \mathrm{BC,OC}; \qquad j = \mathrm{FF,BB}; \qquad k = \mathrm{A,H} \tag{S1}$$

We transform this into a new direct radiative forcing (DRF') using the common set of emissions (E'), then account for the efficacy (f) of the forcing to calculate the direct effective radiative forcing ($DRFe'$). (We employ the efficacies of ref. 3) In A, we also apply a mixing correction (m) of 2 to those AeroCom models that do not account for internal mixing (thereby generating the set of estimates A*). Note that A and H divide BC sources into fossil fuels (FF) and biomass burning (BB); we assume that the *ssNDRF* for BC and OC from contained combustion of biofuels (and thus for CC as a whole) is the same as from fossil fuels. This is a reasonable approximation because the difference in *ssNDRF* between FF and BB is due primarily to the geographic and altitudinal distribution of the aerosol load, and the altitudinal distribution of biofuel-produced aerosols more closely resembles that of fossil fuels than that of open biomass burning.

$$DRF'_{i,j,k} = ssNDRF_{i,j,k} \cdot E'_{i,j} \qquad i = \mathrm{BC,OC}; \qquad j = \mathrm{CC,BB}; \qquad k = \mathrm{A,H} \tag{S2}$$

$$DRF'_{i,j,\mathrm{A}^*} = m_{i,j} \cdot ssNDRF_{i,j,\mathrm{A}} \cdot E'_{i,j} \tag{S3}$$

$$DRFe'_{i,j,k} = DRF'_{i,j,k} \cdot f_{i,j} \qquad i = \mathrm{BC,OC}; \qquad j = \mathrm{CC,BB}; \qquad k = \mathrm{A,A^*,H} \tag{S4}$$

To calculate the indirect RF of BC and OC in A, we first scale the total cloud albedo effect reported by the IPCC ($RFAIE_{\mathrm{tot,IPCC}}$) by the proportion of soot ($L_{\mathrm{POM}} + L_{\mathrm{BC}}$) in the total aerosol load L_{tot} as reported by the models in A. To convert this value into a steady-state normalized RF, we divided by the total carbonaceous aerosol emissions of ref. 10.

$$RFAIE_{\mathrm{CC+BB,A}} = RFAIE_{\mathrm{tot,IPCC}} \cdot (L_{\mathrm{POM,A}} + L_{\mathrm{BC,A}})/L_{\mathrm{tot,A}} \tag{S5}$$

$$ssRFAIE_{\mathrm{CC+BB,A}} = RFAIE_{\mathrm{CC+BB,A}}/E'_{\mathrm{BC+OC,FF+BB}} \tag{S6}$$

For H, we calculate the steady-state indirect radiative forcing from the indirect radiative forcing attributed to each source by H.

$$ssRFAIE_{\mathrm{BC+OC},j,\mathrm{H}} = RFAIE_{j,\mathrm{H}}/(E_{\mathrm{BC},j,\mathrm{H}} + E_{\mathrm{OC},j,\mathrm{H}}) \qquad j = \mathrm{FF,BB} \tag{S7}$$

We then calculate a new indirect radiative forcing ($RFAIE'_{i,j,k}$) using the common set of emissions.

$$RFAIE'_{i,j,k} = ssRFAIE_{i,j,k} \cdot E'_{i,j} \qquad i = \mathrm{BC,OC}; \qquad j = \mathrm{CC,BB}; \qquad k = \mathrm{A,A^*,H} \tag{S8}$$

We adopt the total snow albedo RF reported by H ($RFsnow_{\mathrm{H}}$), which is close to that reported by (11), and apportion it across the common set of emissions to assess the adjusted RF and effective RF of the snow albedo effect.

$$ssRFsnow = RFsnow_{\mathrm{H}} = E'_{\mathrm{BC}} \tag{S9}$$

$$RFsnow'_j = ssRFsnow \cdot E'_{\mathrm{BC},j} \qquad j = \mathrm{CC,BB} \tag{S10}$$

$$RFesnow'_j = RFsnow'_j \cdot f_{\mathrm{snow}} \qquad j = \mathrm{CC,BB} \tag{S11}$$

To calculate the total RF (*RFtotal*) and RFe (*RFetotal*) associated with a source, we sum together the DRF, indirect RF, and snow albedo effect terms.

$$RFtotal'_{j,k} = \sum_{i=\mathrm{BC,OC}} (DRF'_{i,j,k} + RFAIE'_{i,j,k}) + RFsnow'_j \qquad i = \mathrm{BC,OC}; \qquad j = \mathrm{CC,BB}; \qquad k = \mathrm{A,A^*,H} \tag{S12}$$

$$RFetotal'_{j,k} = \sum_{i=\mathrm{BC,OC}} (DRFe'_{i,j,k} + RFAIE'_{i,j,k}) + RFesnow'_j \qquad i = \mathrm{BC,OC}; \qquad j = \mathrm{CC,BB}; \qquad k = \mathrm{A,A^*,H} \tag{S13}$$

Model RC.

For RC, the approach is similar. RC reports the direct RF for BC and the direct plus indirect RF for non-BC aerosols. We apportion a fraction of the latter to OC based on the relative loadings in A, then calculate steady-state normalized RFs (*ssNRF*) based on the emissions of ref. 10.

$$RF_{\mathrm{OC,RC}} = RF_{\mathrm{non-BC,RC}} \cdot (L_{\mathrm{POM,A}})/(L_{\mathrm{tot,A}} - L_{\mathrm{BC,A}}) \tag{S14}$$

$$ssNRF_{i,\mathrm{RC}} = RF_{i,\mathrm{RC}}/E'_{i,\mathrm{CC+BB}} \qquad i = \mathrm{BC,OC} \tag{S15}$$

We then proceed as before.

$$RF'_{i,j,\mathrm{RC}} = ssNRF_{i,j,\mathrm{RC}} \cdot E'_{i,j} \qquad i = \mathrm{BC,OC}; \qquad j = \mathrm{CC,BB} \tag{S16}$$

$$RFe'_{i,j,\mathrm{RC}} = RF'_{i,j,\mathrm{RC}} * f_{i,j} \tag{S17}$$

$$RFtotal'_{j,\mathrm{RC}} = \sum_{i=\mathrm{BC,OC}} RF'_{i,j,\mathrm{RC}} + RFsnow'_j \tag{S18}$$

$$RFetotal'_{j,\mathrm{RC}} = \sum_{i=\mathrm{BC,OC}} RFe'_{i,j,\mathrm{RC}} + RFesnow'_{j} \tag{S19}$$

Model J.

For J, we take a different approach. Ref. 7 reports that the snow albedo effect from all BC sources (ΔT_{snow}) causes a warming of approximately 0.06 K, while over the last three years of a 10 year simulation, the total warming including all effects from CC carbonaceous aerosols ($\Delta T_{\mathrm{CC+snow}}$) was 0.32 K. We apportion the snow albedo effect warming between CC and BB in proportion to their emissions in the model, and subtract the snow warming caused by CC from the total CC warming to determine the CC warming in the absence of the snow albedo effect.

$$\Delta T_{\mathrm{snow},j,\mathrm{J}} = \Delta T_{\mathrm{snow,CC+BB,J}} \cdot E_{\mathrm{BC},j,\mathrm{J}}/E_{\mathrm{BC,CC+BB,J}} \qquad j = \mathrm{CC,BB} \tag{S20}$$

$$\Delta T_{\mathrm{CC-snow,J}} = \Delta T_{\mathrm{CC+snow,J}} - \Delta T_{\mathrm{snow,CC,J}} \tag{S21}$$

To convert the warmings into effective radiative forcings, we calculate an equilibrium climate sensitivity (S) based on the warming in J from a doubling of $\mathrm{CO_2}$, as reported in ref. 8, and a RF change from a $\mathrm{CO_2}$ doubling ($RF_{2\times\mathrm{CO_2}}$) of 3.7 $\mathrm{W\,m^{-2}}$.

$$S = \Delta T_{2\times\mathrm{CO_2},\mathrm{J}}/RF_{2\times\mathrm{CO_2}} \tag{S22}$$

$$RFe_{\mathrm{CC-snow,J}} = \Delta T_{\mathrm{CC-snow,J}}/S \tag{S23}$$

$$RFe_{\mathrm{CC+snow,J}} = \Delta T_{\mathrm{CC+snow,J}}/S \tag{S24}$$

Calculation of illustrative CO_2 emission pathways. To calculate illustrative $\mathrm{CO_2}$ emissions pathways that could be followed to meet a given RF target in 2100, we used a simplified atmospheric and economic model. The model employs a static approximation of the Bern Carbon Cycle model to determine the atmospheric lifetime of $\mathrm{CO_2}$ emissions (22% lasts essentially forever, 26% has a lifetime of 173 years, 34% lasts for 18.5 years, and 19% lasts for 1.2 years) (12, 13). We calculate 19th and 20th century $\mathrm{CO_2}$ emissions to match the observed concentration profile and take as our reference 21st century $\mathrm{CO_2}$ emissions those of the IPCC Special Report on Emissions Scenarios A1B scenario. Following ref. 14, we assume that the cost of emissions reductions relative to the reference level is proportional to the fractional reduction raised to the 2.8th power. We discount costs at 5% annually. The net present value of emission reductions W is thus

$$W = \sum_{i=0}^{9} \exp(-\eta t_i)\left(\frac{x(t_i) - x_0(t_i)}{x_0(t_i)}\right)^{2.8}. \tag{S25}$$

The function $x(t)$ gives the carbon emission rate at time t, whereas $x_0(t)$ gives carbon emissions in the A1B reference scenario. The variables t_i ($i = 0,1,\ldots,9$) demarcate the decades of the twenty-first century. The discount rate (0.05) is given by η. We note that the economic component of this model in particular is extremely simplistic and schematic but argue that a model simplified to this extent is appropriate for constructing metrics to serve as alternatives to Global Warming Potentials.

To calculate an emissions trajectory, we minimize W subject to the constraint that atmospheric concentrations of $\mathrm{CO_2}$ are at the desired value c in 2100. This constraint is calculated as follows. The row vector $\mathbf{M}_i$ represents the changes in atmospheric concentrations of $\mathrm{CO_2}$ at the end of decade i resulting from $\mathrm{CO_2}$ emitted in each decade of the 21st century. Each element $\mathbf{M}_{i,j}$ indicates the change in concentration produced by a decade-long pulse of $\mathrm{CO_2}$ emissions in decade j. The indices i and j run from 0–9, as above. The column vector $\mathbf{X}$ consists of elements $x(t_i)$. The minimization constraint is $\mathbf{M}_9\mathbf{X} = c - c'$, where c' is the modeled concentration of $\mathrm{CO_2}$ at the end of the twenty-first century in the total absence of 21st century anthropogenic emissions (336 ppm). We also impose a "realism" constraint, which requires that $\mathrm{CO_2}$ emissions in 2010–2020 be at least 6.5% greater than in 2000–2010, following the slowest growth rate of all the SRES scenarios (B2).

For RF and $\mathrm{CO_2e}$ calculations, we assume that non-$\mathrm{CO_2}$ GHGs follow their A1B trajectories, as modeled by the National Aeronautics and Space Administration (NASA) Goddard Institute for Space Studies (GISS), and that carbonaceous aerosol emissions decrease from their initial value to their final value starting in 2010 with a half-life of 10 years ($E(t) = E(2100) + (E(2010) - E(2100)) \cdot 2^{-(t-2010)/10}$ for $t > 2010$).

The 2050 A2 and B1 scenarios of ref. 15 have different global BC/OC ratios than at present. To account for this when calculating global carbonaceous aerosol RF, we apply the steady-state normalized RF distributions of H and RC for the "best" case (as the mean of the median of those two models is nearly identical to that of all four models), scaled by 0.92 so that the mean of their medians aligns with the "best" estimate, and apply the distribution of A for the "low" case. Because we have insufficient information to apply J for the "high" case, we scale the H and RC distributions (by 1.56) instead.

We emphasize that this is a highly simplified model and the results should be interpreted cautiously. The difference between scenarios in the timing of the 50% reduction in $\mathrm{CO_2}$ emissions from 2005 levels is, however, fairly robust to changes in the discount rate and the exponential factor in Eq. S1 and can be regarded with greater confidence than the exact shape and timing of the calculated pathways.

1. Schulz M, et al. (2006) Radiative forcing by aerosols as derived from the aerocom present-day and preindustrial simulations. *Atmos Chem Phys* 6:5225–5246.
2. Textor C, et al. (2006) Analysis and quantification of the diversities of aerosol life cycles within AeroCom. *Atmos Chem Phys* 6:1777–1813.
3. Hansen J, et al. (2005) Efficacy of climate forcings. *J Geophys Res* 110:D18104.
4. Hansen J, et al. (2007) Climate simulations for 1880–2003 with GISS modelE. *Clim Dynam* 29:661–696.
5. Ramanathan V, Carmichael G (2008) Global and regional climate changes due to black carbon. *Nat Geosci* 1:221–227.
6. Jacobson M (2002) Control of fossil-fuel particulate black carbon and organic matter, possibly the most effective method of slowing global warming. *J Geophys Res* 107:4410, doi:10.1029/2001JD001376.
7. Jacobson M (2004) Climate response of fossil fuel and biofuel soot, accounting for soot's feedback to snow and sea ice albedo and emissivity. *J Geophys Res* 109: D21201, doi:10.1029/2004JD004945.
8. Jacobson M (2005) Control of fossil-fuel particulate black carbon and organic matter, possibly the most effective method of slowing global warming. *J Geophys Res* 110: D14105, doi:10.1029/2005JD005888.
9. Jacobson M (2006) Effects of externally-through-internally-mixed soot inclusions within clouds and precipitation on global climate. *J Phys Chem A* 110:6860–6873.
10. Bond T, et al. (2004) A technology-based global inventory of black and organic carbon emissions from combustion. *J Geophys Res* 109:D14203, doi:10.1029/2003JD003697.
11. Flanner MG, Zender CS, Randerson JT, Rasch PJ (2007) Present-day climate forcing and response from black carbon in snow. *J Geophys Res* 112:D11202, doi:10.1029/2006JD008003.
12. Joos F, et al. (2001) Global warming feedbacks on terrestrial carbon uptake under the Intergovernmental Panel on Climate Change (IPCC) emission scenarios. *Global Biogeochem Cy* 15:891–908.
13. Forster P, et al. (2007) Changes in atmospheric constituents and in radiative forcing. *Climate Change 2007: The Physical Science Basis*, eds Solomon S, et al. (Cambridge University Press, Cambridge, UK), pp. 130–234.
14. Nordhaus W (2008) *A Question of Balance: Weighting the Options on Global Warming Policies* (Yale University Press, New Haven, CT).
15. Streets DG, Bond TC, Lee T, Jang C (2004) On the future of carbonaceous aerosol emissions. *J Geophys Res* 109:D24212, doi:10.1029/2004JD004902.

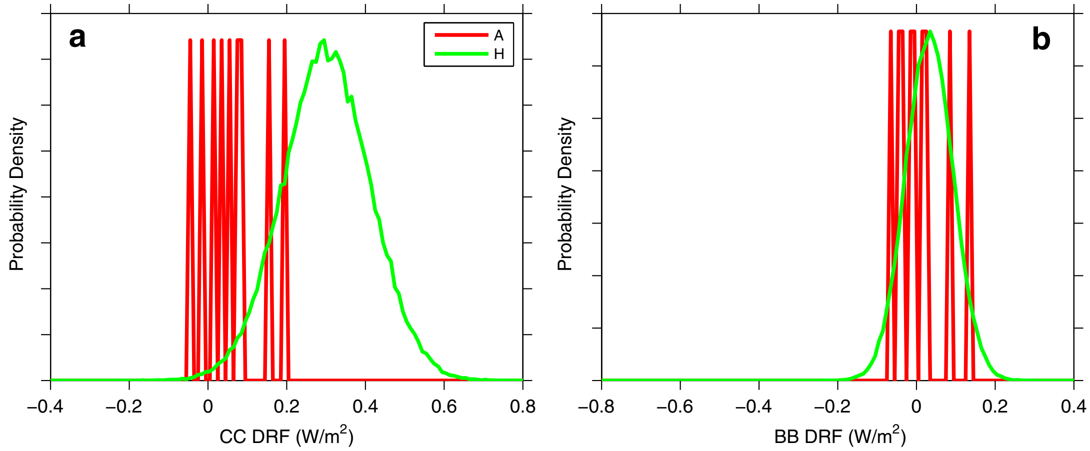

Fig. S1. Probability distributions for the direct RF (DRF) of carbonaceous aerosols from (*A*) contained combustion (CC) and (*B*) biomass burning (BB) from analyses A and H. The spikiness of the curve for A results from the equal weighting of the discrete models in A, which have no reported uncertainties.

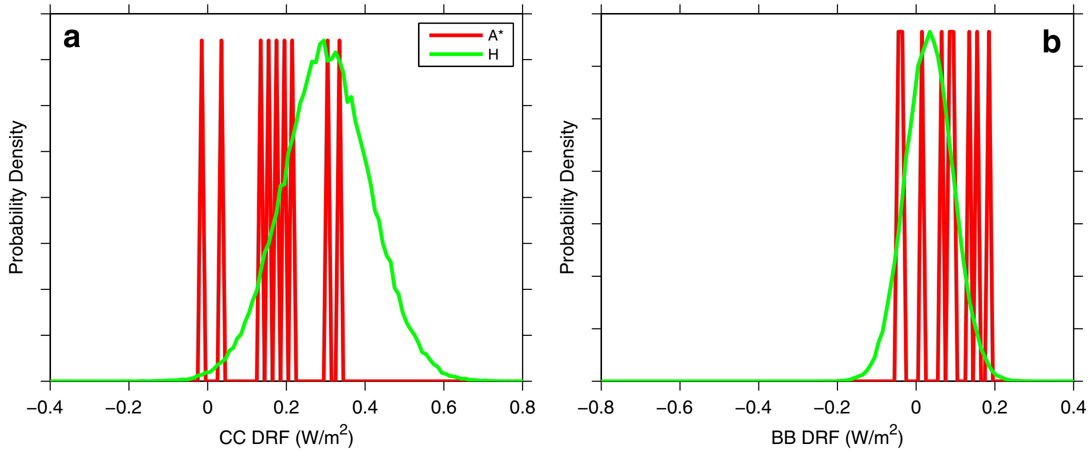

Fig. S2. Probability distributions for the direct RF (DRF) of carbonaceous aerosols from (*A*) contained combustion (CC) and (*B*) biomass burning (BB) from analyses A* and H. The spikiness of the curve for A* results from the equal weighting of discrete models without reported uncertainties.

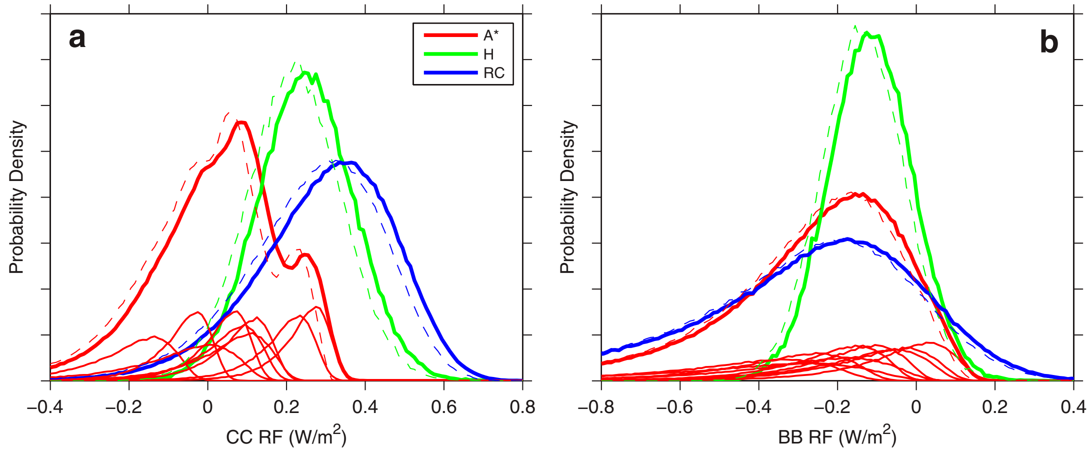

Fig. S3. Probability distributions for the total RF of carbonaceous aerosols from (*A*) contained combustion (CC) and (*B*) biomass burning (BB) from analyses A*, H, and RC. The nine models in A* are shown individually and collectively. Solid lines incorporate the snow albedo effect, assuming that it is caused by CC and BB in proportion to their BC emissions, whereas dashed lines exclude the snow albedo effect.

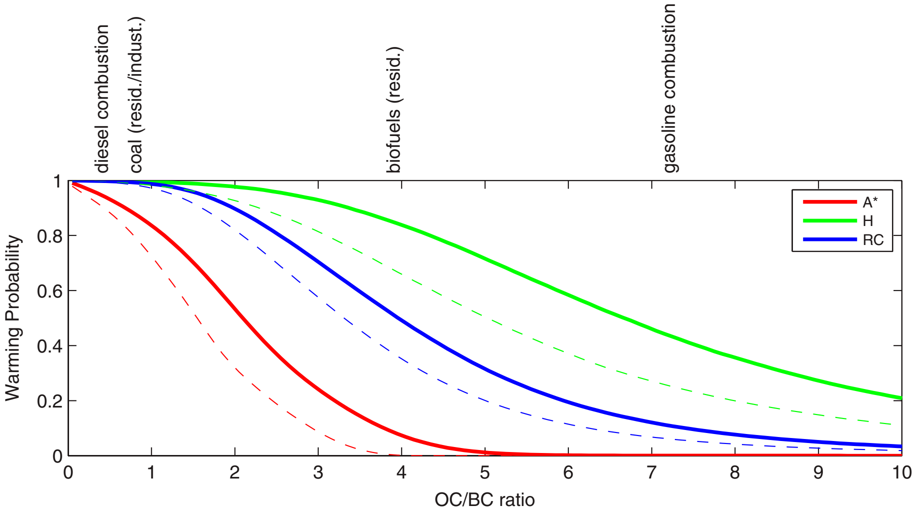

Fig. S4. Probability distribution of the OC/BC threshold above which emissions are no longer net warming, assuming a geographic and altitudinal distribution characteristic of fossil fuel BC sources. Typical OC/BC values of different combustion sources are marked. Solid lines incorporate the snow albedo effect, assuming that it is caused by CC and BB in proportion to their BC emissions, whereas dashed lines exclude the snow albedo effect. Average OC/BC ratios are from (10).

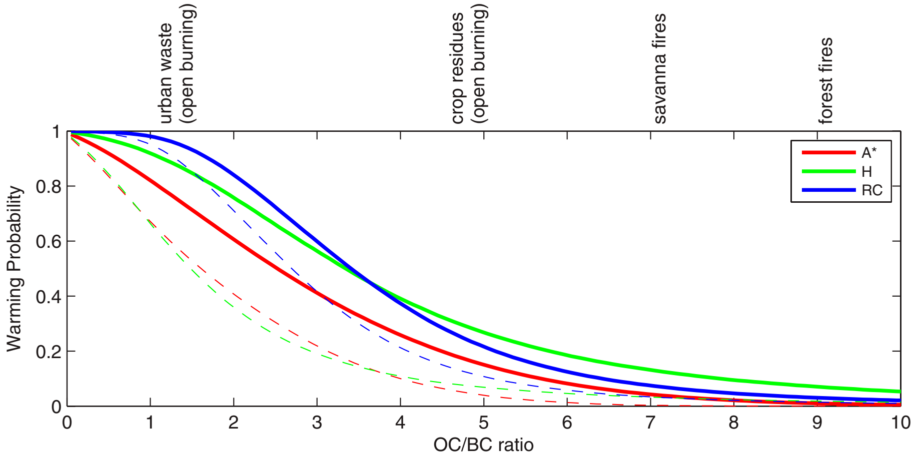

Fig. S5. Probability distribution of the OC/BC threshold above which emissions are no longer net warming, assuming a geographic and altitudinal distribution characteristic of open biomass burning BC sources. Typical OC/BC values of different combustion sources are marked. Solid lines incorporate the snow albedo effect, assuming that it is caused by CC and BB in proportion to their BC emissions, whereas dashed lines exclude the snow albedo effect. Average OC/BC ratios are from (10).

Table S1. Emissions

Study	Ref.	Type	BC emissions	OC emissions
Bond et al.	(1)	Contained combustion	4.6 Tg/y	8.9 Tg/y
		Open biomass burning	3.3 Tg/y	25.0 Tg/y
A	(2)	Fossil fuels	3.0 Tg/y	2.3 Tg/y
		Open biomass burning + Biofuels	3.3 Tg/y	21.0 Tg/y
H	(3, 4)	Fossil fuels	6.6 Tg/y	26.4 Tg/y
	(3, 5)	Open biomass burning	5.5 Tg/y	34.3 Tg/y

1 Bond T, et al. (2004) A technology-based global inventory of black and organic carbon emissions from combustion. *J Geophys Res* 109:D14203, doi:10.1029/2003JD003697.

2 Dentener F, et al. (2006) Emissions of primary aerosol and precursor gases in the years 2000 and 1750, prescribed data-sets for AeroCom. *Atmos Chem Phys* 6:4321–4324.

3 Koch D (2001) Transport and direct radiative forcing of carbonaceous and sulfate aerosols in the GISS GCM. *J Geophys Res* 106:20311–20332.

4 Penner JE, Eddleman H, Novakov T (1993) Towards the development of a global inventory for black carbon emissions. *Atmos Environ* 27A:1277–1295.

5 Liousse C, et al. (1996) A global three-dimensional model study of carbonaceous aerosols. *J Geophys Res* 101:19411–19432.

Table S2. Parameters used in Monte Carlo analysis

Study	Ref.	Parameter	Distribution	Value (where appropriate, median and 90% range, as fitted)
A *	(1)	$DRF_{\mathrm{BC,FF,A}}$	equally weighted	$\{0.12, 0.11, 0.16, 0.15, 0.10, 0.11, 0.18, 0.13, 0.04\}$ $\mathrm{W\,m^{-2}}$
A	(1)	$DRF_{\mathrm{OC,FF,A}}$	equally weighted	$\{-0.06, -0.04, -0.04, -0.04, -0.03, -0.03, -0.02, -0.01, -0.02\}$ $\mathrm{W\,m^{-2}}$
A	(1)	$DRF_{\mathrm{BC,BB,A}}$	equally weighted	$\{0.13, 0.11, 0.16, 0.15, 0.10, 0.11, 0.18, 0.19, 0.04\}$ $\mathrm{W\,m^{-2}}$
A	(1)	$DRF_{\mathrm{OC,BB,A}}$	equally weighted	$\{-0.17, -0.12, -0.12, -0.13, -0.07, -0.11, -0.04, -0.09, -0.07\}$ $\mathrm{W\,m^{-2}}$
A	(13)	$RFAIE_{\mathrm{tot,IPCC}}$	log-normal	$-0.70 (-1.71$ to $-0.29)$ $\mathrm{W\,m^{-2}}$
A	(1)	$L_{\mathrm{tot,A}}$	equally weighted	$\{4.0, 3.0, 5.3, 4.8, 3.4, 2.8, 2.8, 3.2, 3.7\}$ $\mathrm{mg/m^2}$
A	(1)	$L_{\mathrm{BC,A}}$	equally weighted	$\{1.16, 1.12, 1.41, 1.50, 1.00, 1.22, 0.88, 1.84, 1.71\}$ $\mathrm{mg/m^2}$
A	(1)	$L_{\mathrm{POM,A}}$	equally weighted	$\{0.19, 0.19, 0.25, 0.25, 0.16, 0.24, 0.19, 0.37, 0.38\}$ $\mathrm{mg/m^2}$
A	†	$m_{\mathrm{BC,FF,A}}$	see $DRF_{\mathrm{BC,FF,A}}$	$\{2, 2, 2, 2, 1, 2, 1, 1, 1\}$
A	†	$m_{\mathrm{BC,BB,A}}$	see $DRF_{\mathrm{BC,BB,A}}$	$\{2, 1, 2, 2, 1, 2, 1, 1, 1\}$
H	(4)	$RFsnow_{\mathrm{H}}$	normal	0.05 ± 0.05 $\mathrm{W\,m^{-2}}$
H	(3)	$DRF_{\mathrm{BC,FF,H}}$	normal	0.48 ± 0.26 $\mathrm{W\,m^{-2}}$
H	(3)	$DRF_{\mathrm{OC,FF,H}}$	normal	-0.10 ± 0.08 $\mathrm{W\,m^{-2}}$
H	(3)	$RFAIE_{\mathrm{FF,H}}$	normal	-0.20 ± 0.16 $\mathrm{W\,m^{-2}}$
H	(3)	$DRF_{\mathrm{BC,BB,H}}$	normal	0.17 ± 0.14 $\mathrm{W\,m^{-2}}$
H	(3)	$DRF_{\mathrm{BC,BB,H}}$	normal	-0.12 ± 0.10 $\mathrm{W\,m^{-2}}$
H	(3)	$RFAIE_{\mathrm{BB,H}}$	normal	0.30 ± 0.25 $\mathrm{W\,m^{-2}}$
H	(3)	$f_{\mathrm{BC,FF}}$		0.78
H	(3)	$f_{\mathrm{OC,FF}}$		1.00
H	(3)	$f_{\mathrm{BC,BB}}$		0.58
H	(3)	$f_{\mathrm{BC,OC}}$		0.91
H	(4)	f_{snow}		2.7
J	(7)	$\Delta T_{\mathrm{CC+snow,J}}$		0.32 K
J	(7)	$\Delta T_{\mathrm{snow,CC+BB,J}}$		0.06 K
J	(8)	$\Delta T_{2\times \mathrm{CO_2}}$		3.2 K
RC	(5)	$RF_{\mathrm{BC,RC}}$	reversed log-normal	0.90 $(0.42$ to $1.21)$ $\mathrm{W\,m^{-2}}$
RC	(5)	$RF_{\mathrm{non-BC,RC}}$	normal	-2.30 ± 1.15 $\mathrm{W\,m^{-2}}$

*AeroCom models are listed in the order: UMI, UIO_CTM, LOA, LSCE, MPI_HAM, GISS, UIO_GCM, SPRINTARS, ULAQ.

†Whether individual AeroCom models attempted to include the effects of internal mixing was assessed based on primary model papers and on personal communications.